X-716-68-178
PREPRINT

NASA TM X- 63251

MULTIPLE OPERATING POINTS IN PHOTOVOLTAIC POWER SYSTEMS

GPO PRICE $ _____

CSFTI PRICE(S) $ _____

Hard copy (HC) _____

Microfiche (MF) _____

ff 653 July 65

MAY 1968

GSFC — GODDARD SPACE FLIGHT CENTER

GREENBELT, MARYLAND

X-716-68-178
PREPRINT

MULTIPLE OPERATING POINTS IN PHOTOVOLTAIC POWER SYSTEMS

Charles N. Bolton
Space Technology Division, GSFC

and

Paul S. Nekrasov
RCA Astro-Electronics Division

May 1968

GODDARD SPACE FLIGHT CENTER
Greenbelt, Maryland

MULTIPLE OPERATING POINTS IN PHOTOVOLTAIC POWER SYSTEMS

Charles N. Bolton
Space Technology Division, GSFC

and

Paul S. Nekrasov
RCA Astro-Electronics Division*

ABSTRACT

Any space power system has a monotonic voltage-current output characteristic which is determined by the particular electrical properties of its energy source, power-conditioning components, and energy storage devices. Intersection of the output characteristic with a loadline establishes an operating point. When there is more than one intersection, the possibility of multiple operating points exists.

A method of graphic analysis, developed to determine these operating points, was applied to a specific power-subsystem design. Laboratory demonstration has verified the results of the graphic analysis for the specific design chosen.

*Under GSFC Contract NAS5-9668.

CONTENTS

ILLUSTRATIONS

MULTIPLE OPERATING POINTS

IN PHOTOVOLTAIC POWER SYSTEMS

INTRODUCTION

Designers of power supplies for space use have always been concerned with the possibility of certain anomalous behavior in photovoltaic power systems. The origin of this behavior is attributed to the so-called multiple operating points which may cause a condition known as lockup.

Any space power system has a monotonic voltage-current output characteristic which is determined by the particular electrical properties of its energy source, power-conditioning components, and energy storage devices. Intersection of the output characteristic with a loadline establishes an operating point. When there is more than one intersection, the possibility of multiple operating points exists.

This document describes this problem in detail and gives the results of a detailed graphic analysis of a hardware-implemented space power system with a pulsewidth-modulated (PWM) regulator. It also gives the results of a limited power system experiment.

The authors investigated only those systems that use PWM load-voltage regulation. At the input terminals of these regulators, a constant loadline is roughly hyperbolic in the I-V plane; therefore, more than one intersection with the system output characteristic may exist.

The Nimbus B spacecraft power system (Figure 1) used as a model was designed by RCA under NASA/GSFC contract NAS5-9668. It uses an advanced voltage regulator (AVR) with PWM techniques which RCA developed for GSFC under contract NAS5-3248. The system also contains nickel-cadmium batteries protected by a tapered-charge mechanism, voltage limiters to limit array bus-voltage excursions, and an oriented solar array to maintain energy balance under specified load conditions.

MULTIPLE OPERATING POINTS AND LOCKUP

Multiple points on a power system output characteristic can satisfy the constant power-load requirements of certain magnitudes.* In many cases,

*Koerner, T. W.: Static Power Conversion for Spacecraft. Astronautics and Aerospace Engineering, May 1963.

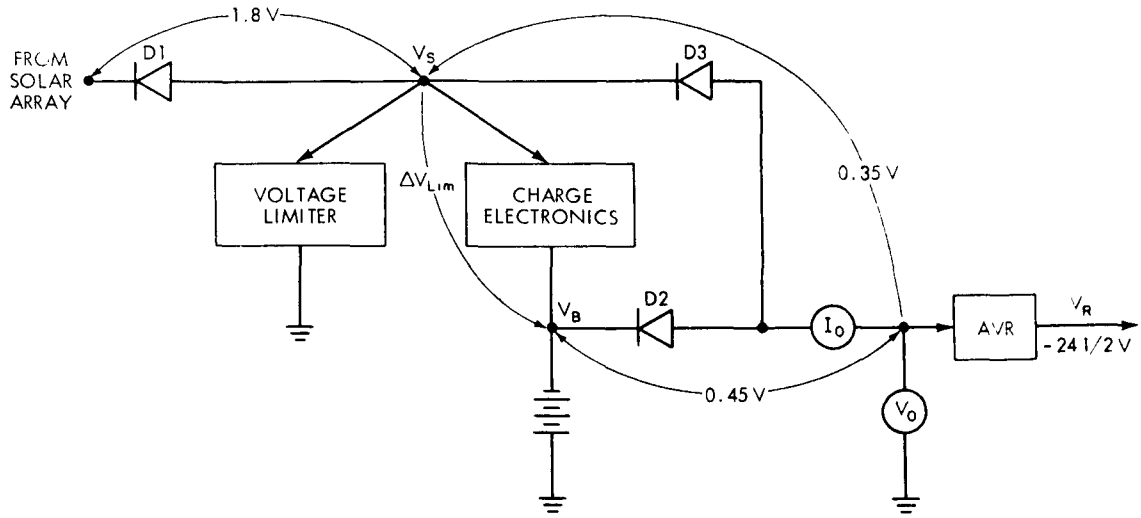

Figure 1. Nimbus B Power System, Simplified Block Diagram

certain fixed loadlines intersect the output characteristic two, three, or even five times. Assuming that a power system can operate from any part of its I-V output characteristic and that the only limitation is that the required load power equal the source power available, as many operating points are possible as there are intersections.

The problem of lockup is frequently encountered when the possibility of multiple operating points exists. When several operating points are possible, some are usually less desirable than others. For instance, a constant-power hyperbola may intersect the composite output I-V characteristic of a power system in the battery charge-voltage region at one point, and in the discharge-voltage region at another. The latter, a lockup condition, would create a less favorable spacecraft energy balance.

Figure 2 shows various possible multiple operating points. The curve, I_{sc}-o-b-v_{oc}, defines the solar-array output characteristic; o-d, the battery-discharge characteristic; and o-l-c, the battery charge plus charge electronics. The o-t-h curve also defines the battery charge plus charge electronics with a lower charge-current condition; maximum charge limiting occurs on the l-c (t-h) part of the curve.

The composite power-system output characteristic at the PWM regulator input is d-o-l-c. The constant-power lines, P_1 < P_2 < P_3 < P_4, show the load characteristics at the same point in the power system. The points where a loadline intersects d-o-l-c are the possible power-system operating points at the regulator input. Loadlines and output characteristics are described in more detail later in the text.

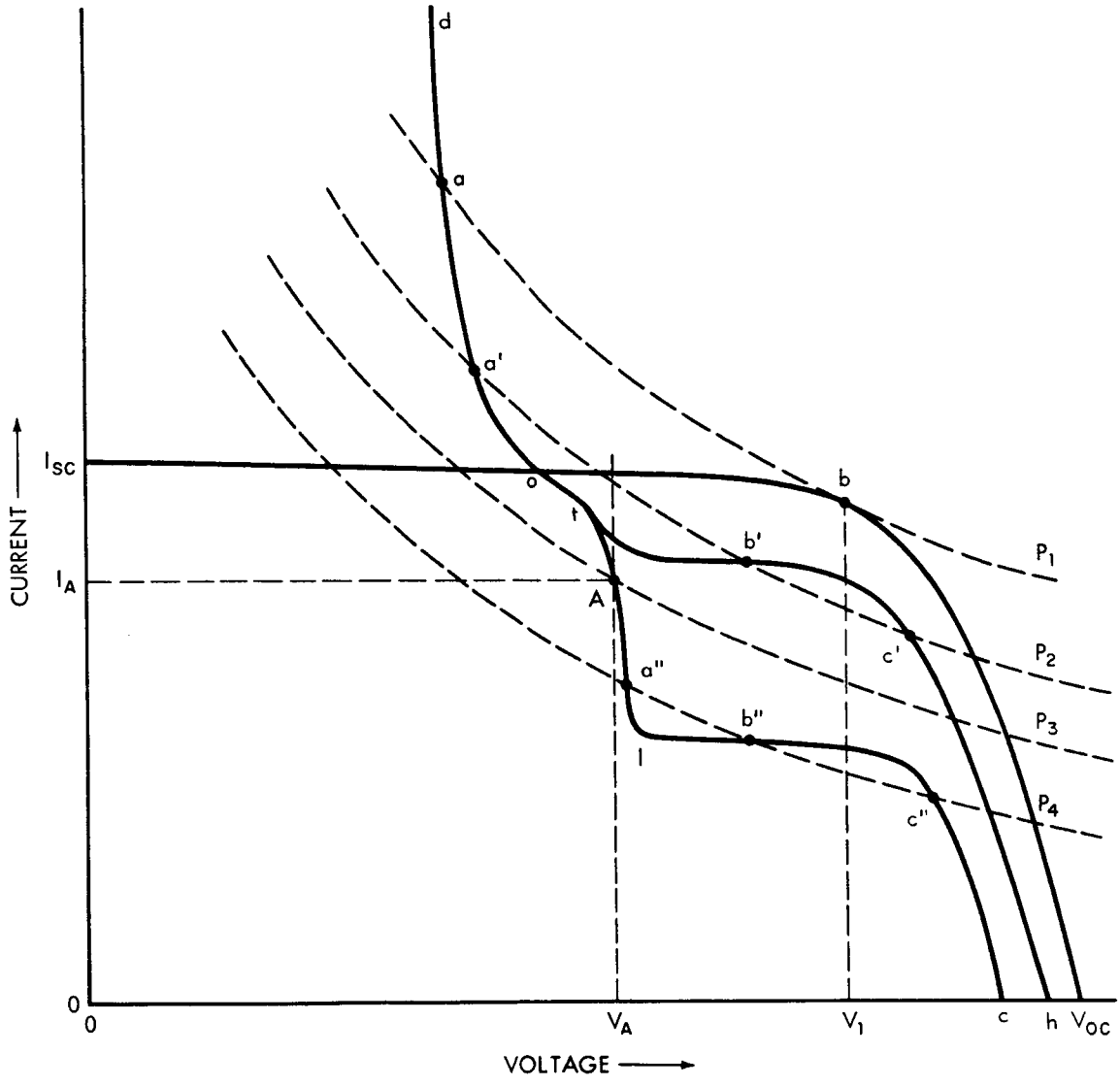

Figure 2. Multiple Operating Points

In Figure 2, load demand P_3 results in a hyperbola which intersects the power-system output characteristic d-o-l-c at point A only. Therefore, if diodes are ideal and power-system shunt losses are negligible, regulator input voltage $V_o = V_A$ and input current $I_o = I_A$, the battery is under charge, and the charge current is the difference between the array current at V_A (roughly equal to I_{sc}) and I_A.

If the power demand is P_4, the P_4 loadline intersects the power-system output characteristic three times; i.e., at a", b", and c". Assuming that the three operating conditions are equally likely, b" and c" are essentially the

same to the extent that in each the charge electronics are limiting, allowing maximum recharge. The third possibility is a" : Although the battery is still under charge, the charge electronics are not limiting; therefore, the amount of recharge is lower than that of the other two possible operating points. For this reason, operating at a" is less advantageous and, if operated at a" , the power system will be in a state of minor lockup.

To illustrate a more drastic lockup condition, assume that the power-system characteristic is d-o-t-h and the power demand is P_2. In the previous example (P_4 and d-o-l-c), the difference between desired operation and lockup was either more charge or less charge, respectively, but charge did occur in both. In this example (P_2 and d-o-t-h), both b' and c' have full charge, as did b" and c" ; but a', unlike a" , has battery discharge. Therefore, it is less desirable to be in the a' lockup condition than the a" lockup condition.

Finally, assume that the power demand at the PWM regulator input is P_1 so that the load requirement matches the solar-array capability shown by point b. Point a is not an example of lockup because it is the only point at which the system can operate if the demand is P_1 . Although the array can supply P_1 at voltage V_1 , the presence of V_1 at the input of a commonly used series-pass dissipative charge-electronics circuit would cause the flow of charge current to equal the current difference between curves o-v_{oc} and o-l-c (or o-t-h) at V_1 . If part of the array output to the battery were diverted, the available load power would be less than P_1 and the regulator action would kick the operating point over to a, causing the battery to discharge. In other words, a possible operating points exists only where the loadline intersects the power-system output characteristic, such as at d-o-l-c.

The foregoing discussion attempts to show what is, and what is not, considered to be a possible lockup condition. A distinction is also made between two cases of lockup: (1) where the recharge is merely lower than the system capability indicates, and (2) where the ability of the power system to both supply the load and charge the battery is not fully utilized, resulting in a net discharge.

The exact graphic analysis of the Nimbus B power system developed in the following section is an example of a typical case in which multiple intersections can occur.

NIMBUS B POWER SYSTEM OPERATING CHARACTERISTICS

The second-generation version of the Nimbus B power system includes an AVR load-voltage regulator, with efficiency vs load plots as shown in Figure 3,

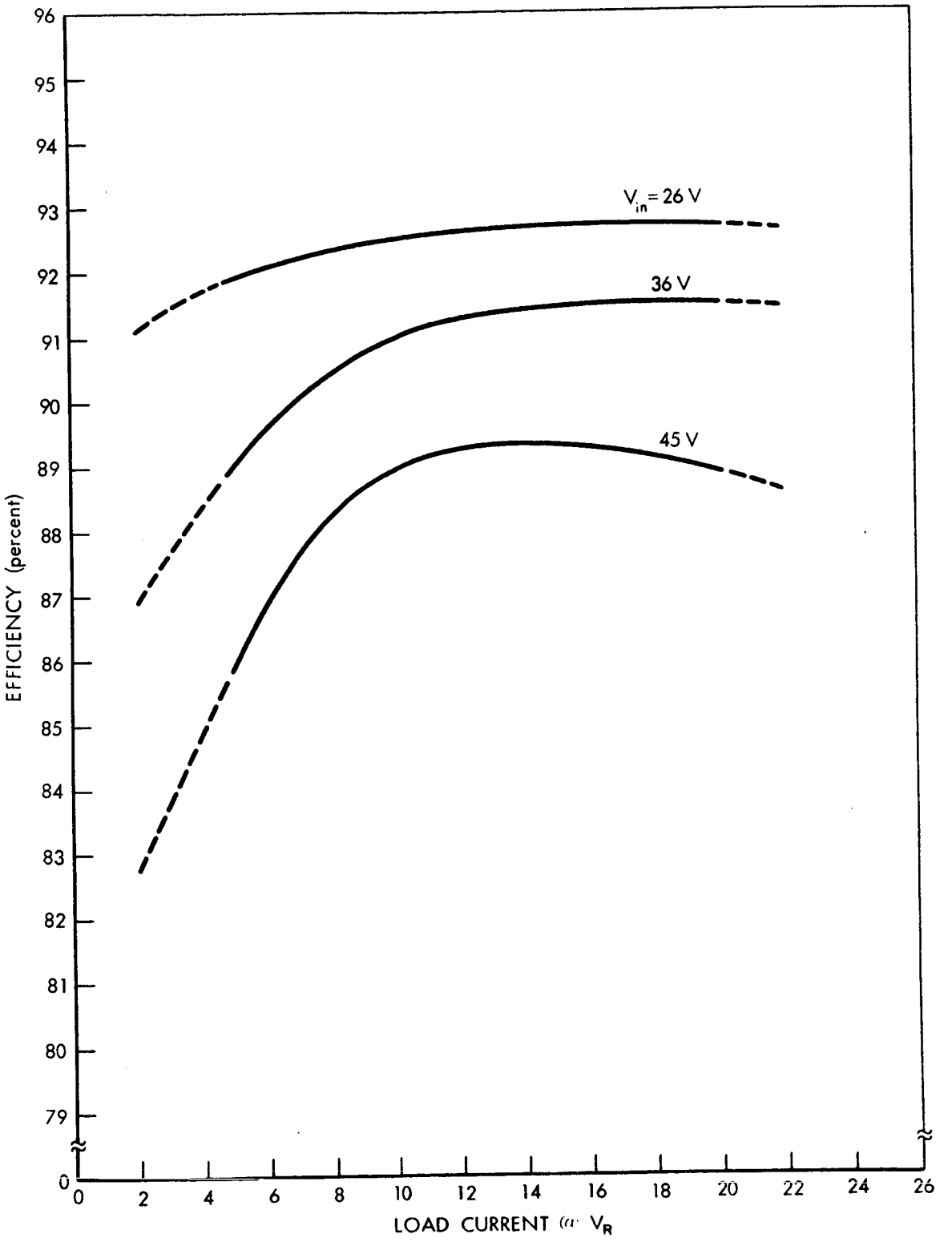

Figure 3. AVR Efficiency vs Load at +25° C

and an improved dissipative tapered-charge electronics/current-limiter circuit (Figure 4). Other significant component data are:

- Voltage-limiter threshold-voltage characteristic (Figure 5)
- Nominal end-of-life I-V curve of a typical Nimbus B nickel-cadmium storage cell (Figure 6)
- Solar-array output characteristic based on worst-case design criteria at the predicted steady-state cell temperature of +40°C (Figure 7)

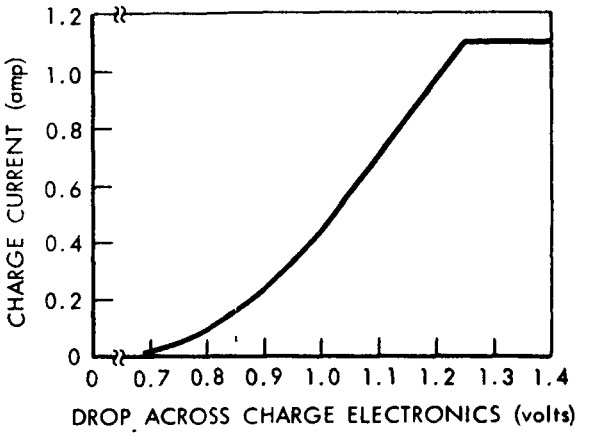

Figure 4. Nominal Charge-Electronics Limiting Characteristic

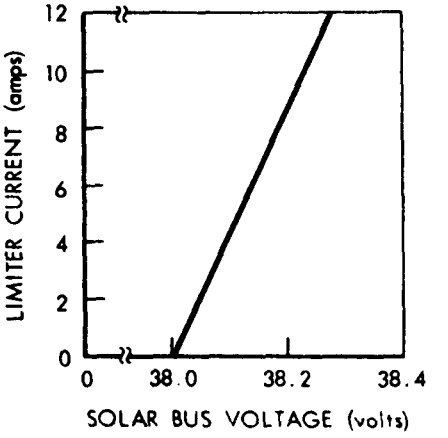

Figure 5. Voltage-Limiter vs Threshold Voltage

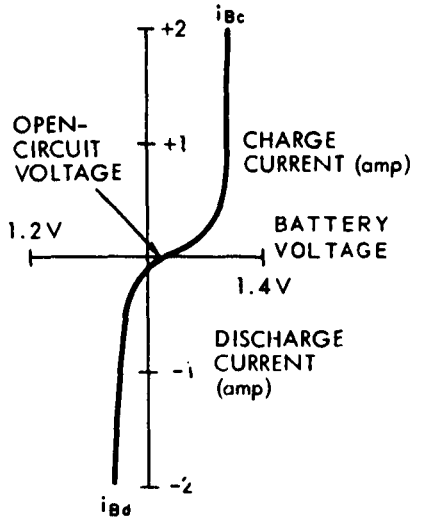

Figure 6. End-of-Life I-V Curve of Typical Nimbus Ni-Cad Storage Cell

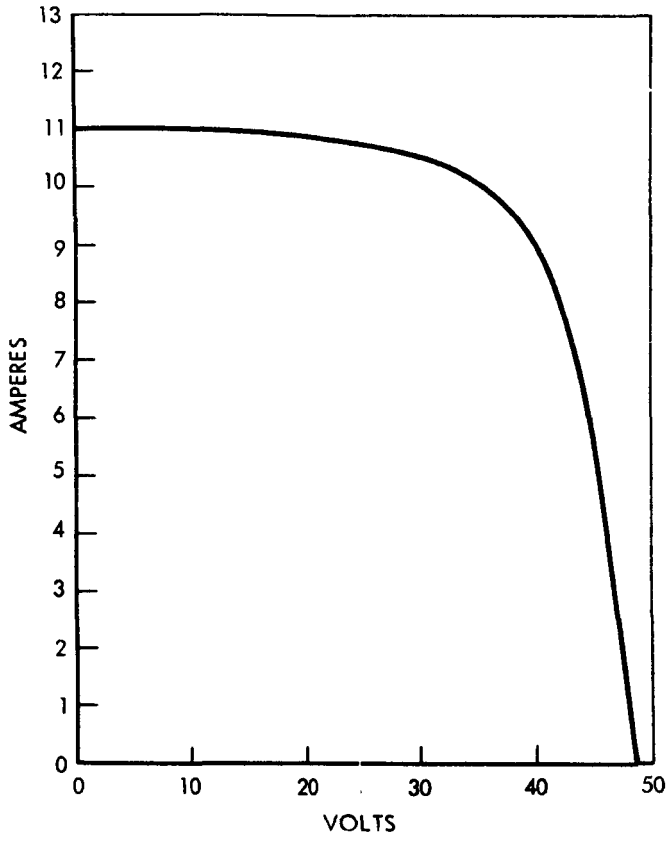

Figure 7. Worst-Case Predicted Output of Nimbus B Solar Array at +40° C (12 months in orbit)

This section contains a detailed graphic analysis of the system. The advanced voltage regulator (AVR) input terminals were selected as the most convenient reference point for evolving the details of the analysis. At this point, it is most convenient to investigate the power-system output capability and to compare it with the load demand which appears at AVR terminals as a family of curves approximating hyperbolas on an I-V plot. The analysis reflects exact operating conditions when possible; approximations are made only when necessary to examine the system in a state of typical, rather than all possible, conditions of life, temperature, and state of charge.

Figure 1 shows specific conditions which are applicable to Nimbus B. Although only one battery is shown, the system contains eight battery modules. Expressed on a per-module basis, the system is subject to shunt-current drains of 22 ma at voltage V_S, 22 ma at V_B, and 25 ma at V_R. These currents are necessary for operating the power-system electronics and, to the extent that they are not delivered as either load or charge, are considered as a loss.

The following procedure is used to determine end-of-life output characteristics at the AVR input terminals.

Solar Array

Refer to Figure 8. Array output at cell level (array side of blocking diodes D1) is as shown in Figure 7. To reflect true conditions at AVR input (I_o, V_o, Figure 1), the following shifts are applied to the solar-cell output curve over the significant voltage range of power-system operation:

Voltage Shift—The entire curve is shifted to the left by the amount of 1.8 + 0.35 = 2.15 volts, the total voltage drop from solar cells to AVR input terminals.

Current Shifts—First, the entire curve (shifted as above) is further shifted downward by the amount of total shunt-current loss at V_S (i.e., 22 ma × 8 modules = 0.176 ampere). Second, part of the resultant curve from battery open-circuit voltage and to the right is shifted by the amount of total loss at V_B, or another 0.176 ampere.

The array-output characteristic thus shifted is further altered to reflect the shunt limiter. The nominal shunt-limiter characteristic (Figure 5) shows the circuit turning on at 38 volts; reflected to AVR terminals, the turn-on voltage is reduced by the drop through the D3 diode path (i.e., 38 - 0.35 = 37.65 volts). Therefore, at AVR input terminals, the array output is limited at turn-on to 37.65 volts and is labeled "s" in Figure 8, where a curve may now be drawn through points i-o-s to show the reflected array output.

Point s (Figure 8) is located at I_o = 8.6 amperes, corresponding to 38.2 volts on the nominal shunt-limiter characteristic. At AVR input, this becomes 38.2 - 0.35 = 37.85 volts, shown as point v in Figure 8 where the reflected effective array output is now completed as i-o-s-v.

Reflected Discharge Characteristic

Three items are significant:

1. The battery discharge voltage is reduced at AVR input by the amount of voltage drop through the D2 path (0.45 volt).

2. There are 23 storage cells in series.

3. When in discharge, the eight batteries deliver a total shunt loss at V_B of 0.176 ampere.

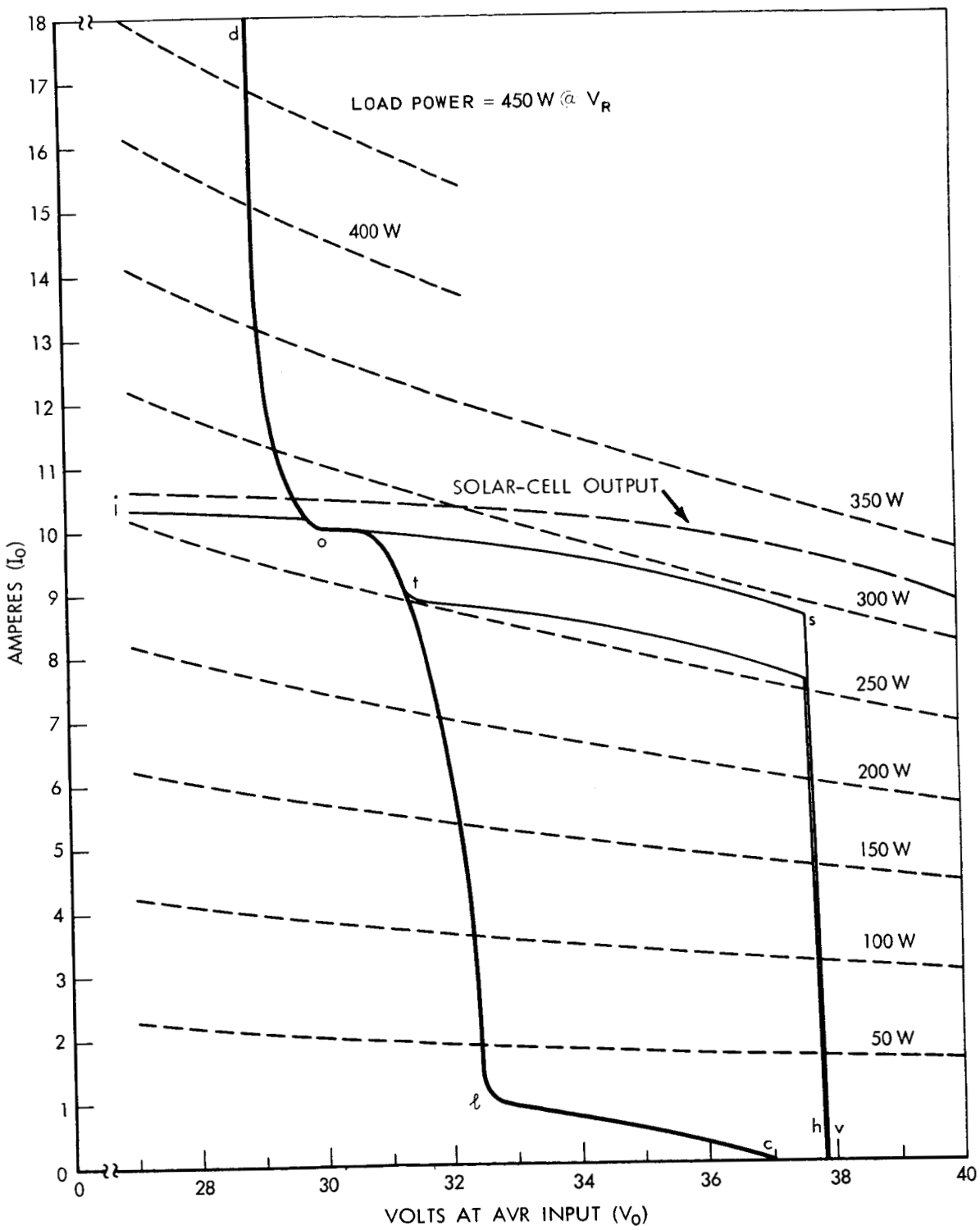

Figure 8. End-of-Life (12 months) Nimbus B I-V Characteristics at AVR Input

In the following table, the first two columns give the discharge voltage and current of a nominal Nimbus B storage cell (Figure 6); the third column, the voltage at AVR input; and the last column, the net total current through discharge path D2.

V_{Bd} (volts per cell)	i_{Bd} (amperes)	V_o^* (volts)	$I_o^\dagger$ (amperes)
1.318	0.0	29.85	
1.295	0.15	29.3	1.02
1.283	0.4	29.1	3.02
1.28	0.6	29.0	4.62
1.279	0.7	28.95	5.42

*$V_o = 23\ V_{Bd} - 0.45$ volts
†$I_o = 8\ i_{Bd} - 0.176$ amperes

Discharge characteristic o-d is generated at corresponding voltages (Figure 8) by graphically adding current values in the last columns to i-o.

Reflected Battery Charge and Charge Electronics Characteristics

In the following table, the first two columns give the per-cell charge voltages and currents from Figure 6. The third column gives the voltage difference between the charge electronics input and the battery terminals corresponding to charge current i_{Bc}, taken from the nominal charge electronics characteristic (Figure 4). The fourth column gives the charge electronics input voltage, V_s, reflected to the AVR input (i.e., the sum of battery charge voltage and limiter drop is reduced by the drop through D3). The last column gives total battery charge current.

Overall characteristics in the last two columns are constructed in Figure 8 by subtracting $8\ i_{Bc}$ from o-s at corresponding voltages, whereupon curve o-ℓ' is drawn. Beyond point ℓ' the characteristic is derived by subtracting the limiting value of $8\ i_{Bc}$; i.e., 8.8 amperes from o-s-v. The entire power-system output characteristic during charge is therefore o-ℓ'-c.

V_{Bc} (volts per cell)	I_{Bc} (amperes)	ΔV_{lim} (volts)	V_o^* (volts)	$8\, i_{Bc}$ (amperes)
1.318	0.0	0.7	30.7	
1.342	0.16	0.85	31.35	1.28
1.36	0.35	0.96	31.9	2.8
1.366	0.54	1.04	32.1	4.32
1.368	0.77	1.13	32.3	6.16
1.37†	1.10†	1.25†	32.45†	8.8†

*$V_o = 23\, V_{Bc} + \Delta V_{lim} - 0.35$ volts
† Represents the current-limiting condition

Similarly, o-t-h shows trickle charge condition; i.e., total charge to all eight batteries of the Nimbus B storage system is assumed to be limited to 1 ampere.

The entire power-system output characteristic at the input to the AVR, or any regulator, is d-o-ℓ-c. The method of constructing the beginning-of-life characteristic, d'-o'-ℓ'-c' (Figure 9), is identical to that previously outlined for the end-of-life characteristic in Figure 8.

Fixed Loadlines at AVR Input

AVR input current I_o equals

$$I_o = \frac{P_L + P_{loss}}{e_c\, V_o},$$

where

P_L = load power (watts) at the regulated bus voltage V_R (= 24.5 volts),

P_{loss} = shunt-current loss at V_R expressed as 25 ma per module × 8 modules × 24.5 volts (about 5 watts),

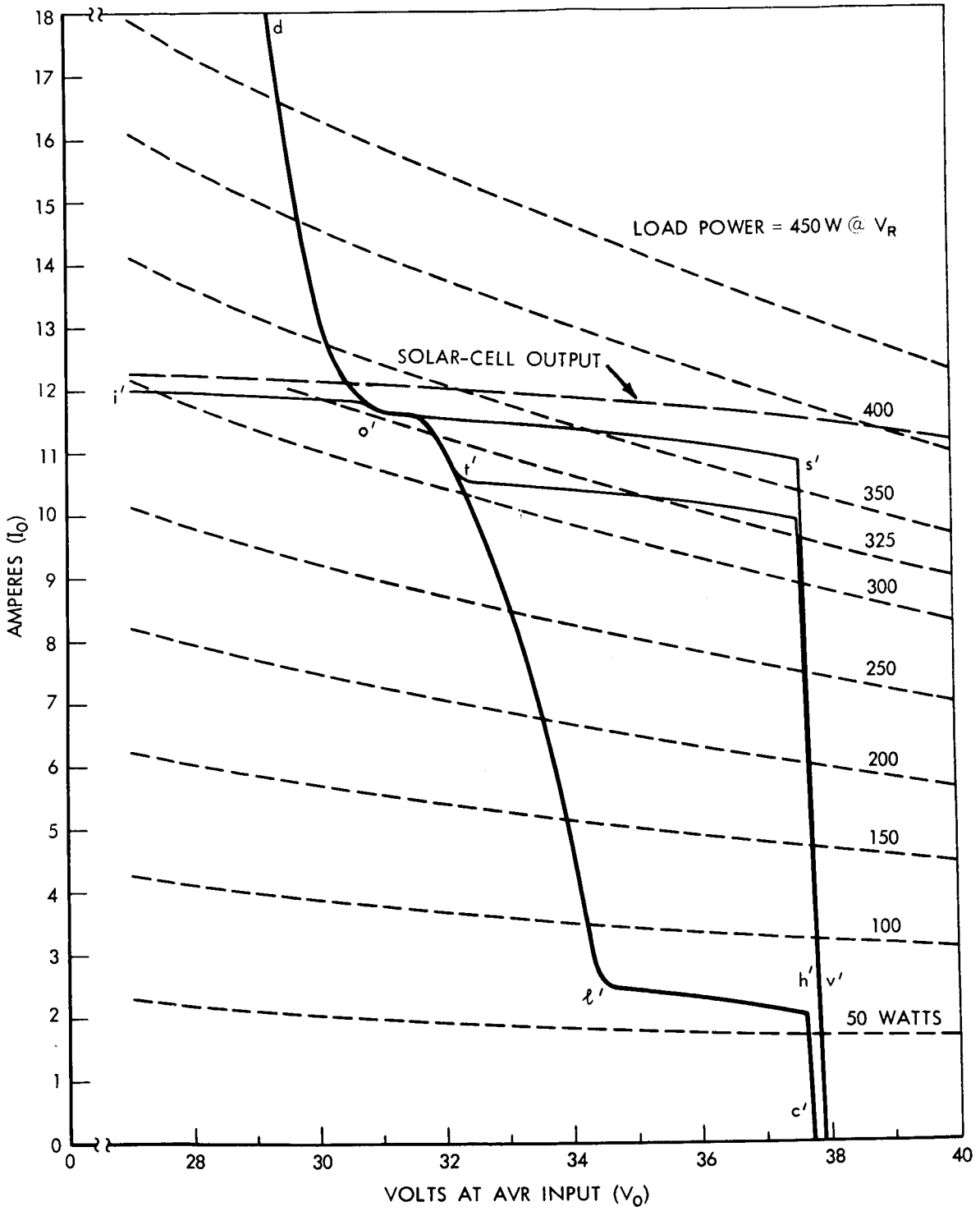

Figure 9. Beginning-of-Life Nimbus B I-V Characteristics at AVR Input

e_c = AVR efficiency factor (function of load current and input voltage (Figure 3)),

V_o = AVR input voltage.

Values of V_o, I_o are the dotted curves plotted in Figures 8 and 9 for fixed loads P_L in 50-watt steps.

DISCUSSION

Now that the multiple operating points have been discussed, look again at Figures 8 and 9. Figure 9 shows the beginning-of-life conditions. When all batteries are capable of being fully charged, the power-system output characteristic is d'-o'-ℓ'-c'. Because none of the fixed loadlines intersects this characteristic more than once, it appears that lockup will not occur under the conditions shown.

As the batteries become recharged and the individual battery charge currents taper off to a low value, the ℓ'-c' portion of the output characteristic will move up and multiple intersections will occur, given fixed loads of approximately 250 watts or more, until all eight batteries are in trickle charge condition. When all eight batteries are in trickle charge condition, the system output characteristic will be d'-o'-t'-h'. Because the 325-watt loadline (Figure 9) intersects the system output characteristic three times, a minor lockup is possible, as in the P_4 condition at a" in Figure 2. The lockup condition described is not likely to occur until the charge to the batteries is reduced to a lower level, as it will be when the batteries are near the point of full recharge.

Figure 8 shows the end-of-life conditions. Close examination of the plots shows an even smaller chance of lockups than at the beginning-of-life, primarily because of the decreased voltage capability of the degraded array.

Finally, in order to establish whether all multiple operating points indicated by graphic analysis of the loadlines are stable and feasible, Nimbus solar panels were tested in outdoor illumination with the solar-panel electrical output connected to the remainder of the power subsystem. A variable load was delivered by an AVR. During the test, the condition of all batteries in trickle charge was simulated so that the multiple operating points could occur.

Figure 10 illustrates the results of this test. The a-b-c-d curve is the output characteristic analogous to d-o-t-h in Figures 2, 8, and 9. During the test, the stable operating points depended on load magnitude and on direction of

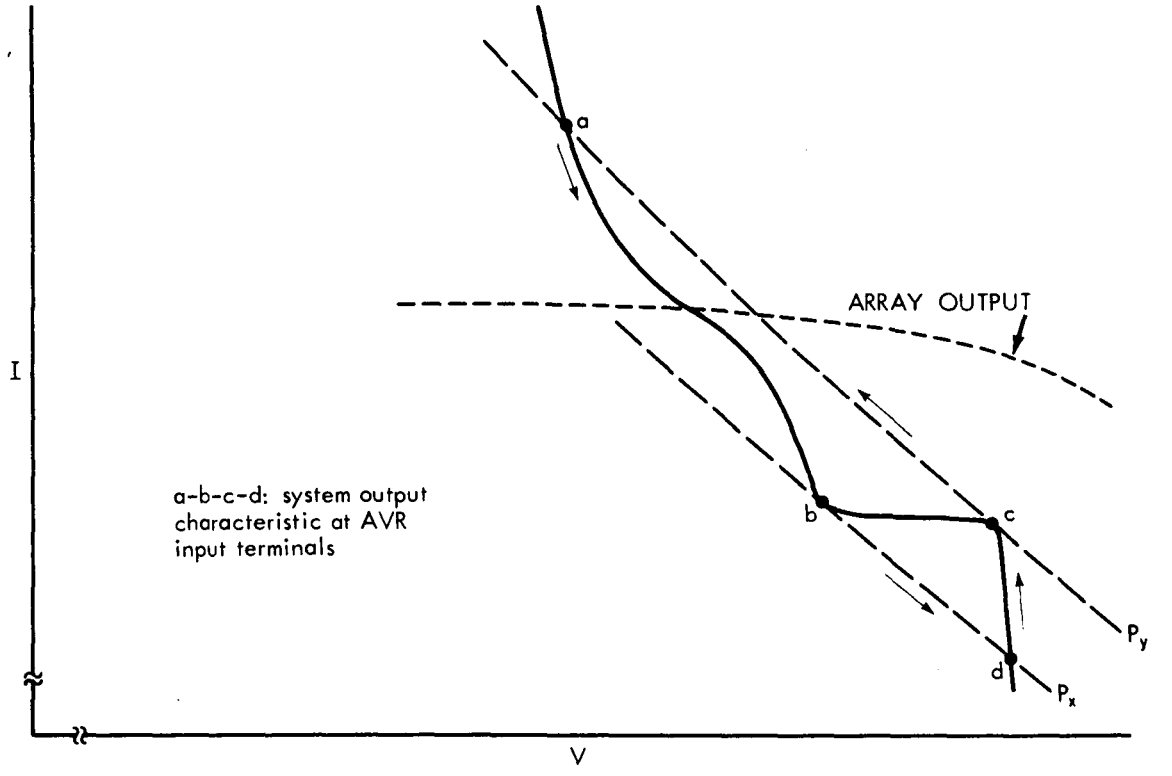

Figure 10. Stable Operating Points

the load change as shown in Figure 10. With a load adjusted to a magnitude less than P_x, the operating point was located along the reflected voltage-limiter characteristic, c-d. Load magnitude was adjusted upwards to P_y, and the operating point moved along c-d to point c. Slight load increase above P_y caused the operating point to switch over from c to a as shown by the arrow. When the load was again reduced, the operating point moved downwards along a-b. Reduction below P_x resulted in a switchover of the operating point from b to d.

The apparent hysteresis effect observed experimentally covers a range of approximately 6 or 7 volts along the voltage axis and occurs over a load range of approximately 22 watts. This effect is in agreement with the graphic analysis of the system described previously. Stable operating points, such as b' in Figure 2, could not be achieved.

CONCLUSIONS

Examination of specific operating conditions indicates that a significant lockup is unlikely in a typical situation such as that illustrated by the Nimbus B

power system. Chances of a minor lockup appear to be influenced mainly by the slope of the charge-controller characteristic when limiting, relative to the slope of the nearest fixed loadline. The most probable conditions for this type of lockup occur when the limiting portion of the charge-controller characteristic is horizontal as shown in Figure 4, and when operation is carried on along the constant-current part of the array curve.

In the Nimbus B power system, undesirable operating conditions can exist over a load range of approximately 250 watts at the low end and 350 watts at the high end. Within this broad range is a narrow range of up to 25 watts (less at end-of-life) over which multiple operating points can occur. Location of the narrow range within the broad range is dependent on the time of life and state of charge of the eight batteries in the system.

In the Nimbus B power system, overall effects of the multiple-operating-point phenomenon are not serious because:

1. Chances of multiple operating points occurring at end-of-life are very small, at least under the conditions of the assumed component characteristics.

2. The effect of an undesirable operating point is merely a moderate decrease in the recharge rate.

3. The effect does not occur until the charge to several batteries has tapered. This condition normally occurs near the point of full recharge.

ACKNOWLEDGMENT

The authors acknowledge the contribution of R. Rasmussen of the Spacecraft Design Department, RCA/AED, in conducting the experiment (Figure 10).